Inorganic Chemistry

Article

pubs.acs.org/IC

Homochiral Metal–Organic Frameworks with Enantiopure Proline Units for the Catalytic Synthesis of β-Lactams

Zhong-Xuan Xu,[†,‡] Yan-Xi Tan,[†] Hong-Ru Fu,[†] Juan Liu,[†] and Jian Zhang*[,†]

[†]State Key Laboratory of Structural Chemistry, Fujian Institute of Research on the Structure of Matter, Chinese Academy of Sciences, Fuzhou, Fujian 350002, People's Republic of China

[‡]Department of Chemistry, Zunyi Normal College, Zunyi, 563002, People's Republic of China

Supporting Information

ABSTRACT: Two enantiopure organic ligands integrating flexible proline units and rigid isophthalate units have been rationally designed and employed for the construction of four homochiral porous metal–organic frameworks (MOFs), respectively. One pair of these MOFs is used as heterogeneous catalysts to construct β-lactam derivatives by oxidative coupling reactions.

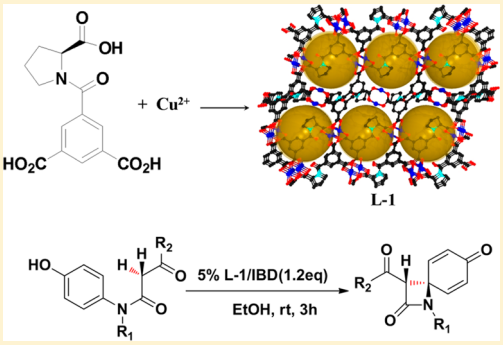

INTRODUCTION

Current interest in homochiral metal–organic frameworks (HMOFs) is rapidly expanding, because of their potential applications in enantioselective processes.[1−4] The most effective method to synthesize HMOFs is to select an enantiopure ligand as the primary linker to impart homochirality to the frameworks.[1−3] Rational design of enantiopure ligands is very important for the construction of HMOFs with special functions. For example, the coordination fashion of enantiopure ligands should not only determine the homochiral environment, but also control the framework stability and the generation of active sites.[5] So far, determining how to design the new enantiopure ligands and then construct functional HMOFs is still a huge challenge for chemists.

Natural amino acids may be the inexpensive and ideal enantiopure linkers for the formation of HMOFs.[3] However, the pore sizes of these resulting HMOFs are always limited by the flexible nature of amino acids. Adding rigid auxiliary ligands (e.g., 4,4′-bipyridine) to support the porous structures of such HMOFs is an effective approach,[3,6] and another typical way is to modify the functional groups (−NH_2 or −COOH) of amino acids with suitable aromatic parts.[7] Although some efforts focus on the synthesis of HMOFs based on the derivatives of amino acids,[8] large porous structures integrating catalytic properties remain rarely explored.

Inspired by the outstanding MOF structure, **HKUST-1**,[9] we try to modify the 1,3,5-benzenetricarboxylate ligand in **HKUST-1** into an enantiopure linker via adding one proline group (see Scheme 1). It is well-known that proline and its derivatives are very promising catalysts for asymmetric organic synthesis.[10] In addition, the remaining isophthalate unit of the ligand tends to connect paddle-wheel type units (e.g., $Cu_2(COO)_4$) into large cages, which is a very successful building strategy on MOFs.[11] Such a combination of enantiopure proline and isophthalate unit may provide a new and feasible approach to design and construct HMOFs with large porosity and specific functions.

In this contribution, we report the successful synthesis of a pair of enantiopure 5-(2-carboxypyrrolidine-1-carbonyl) isophthalic acid (denoted as (*S*)-H_3PIA and (*R*)-H_3PIA) (Scheme 1) and two enantiomeric pairs of HMOFs, namely, $[Cu_3((S)\text{-PIA})_2(1,4\text{-dioxane})(H_2O)_2]\cdot 2(1,4\text{-dioxane})\cdot H_2O$ (**L-1**), $[Cu_3((R)\text{-PIA})_2(1,4\text{-dioxane})(H_2O)_2]\cdot 2(1,4\text{-dioxane})\cdot H_2O$ (**D-1**), $[Cu_4((S)\text{-PIA})_{2.5}(H_2O)_3]\cdot x(\text{guest})$ (**L-2**) and $[Cu_4((R)\text{-PIA})_{2.5}(H_2O)_3]\cdot x(\text{guest})$ (**D-2**).[12,13] All HMOFs exhibit three-dimensional (3D) porous structures containing paddle wheel $[Cu_2(COO)_4]$ units linked by the enantiopure ligands, and large cages are presented in these homochiral structures. The structural details of **L-1** and **L-2** are described below.

EXPERIMENTAL SECTION

General Procedures. All of the reagents and solvents used in reactions were purchased from Energy-Chemical, Sigma–Aldrich, Acros, TCI, or Alfa Aesar and used without purification, unless otherwise indicated. ^{1}H NMR (400 MHz) and ^{13}C NMR (100 MHz) spectra were recorded in $CDCl_3$ (δ 7.26) or DMSO (δ 2.49) solutions using a Bruker Model Avance 400 spectrometer. Elemental analyses and mass spectra were performed by the analysis center of our institute. Chemical shifts are reported as δ values in parts per million (ppm), relative to tetramethylsilane (TMS) for all recorded NMR

Received: September 12, 2014
Published: October 31, 2014

   dx.doi.org/10.1021/ic501849g | Inorg. Chem. 2014, 53, 12199−12204

Scheme 1. Synthetic Routes to the Ligands (*S*)-H_3PIA and (*R*)-H_3PIA

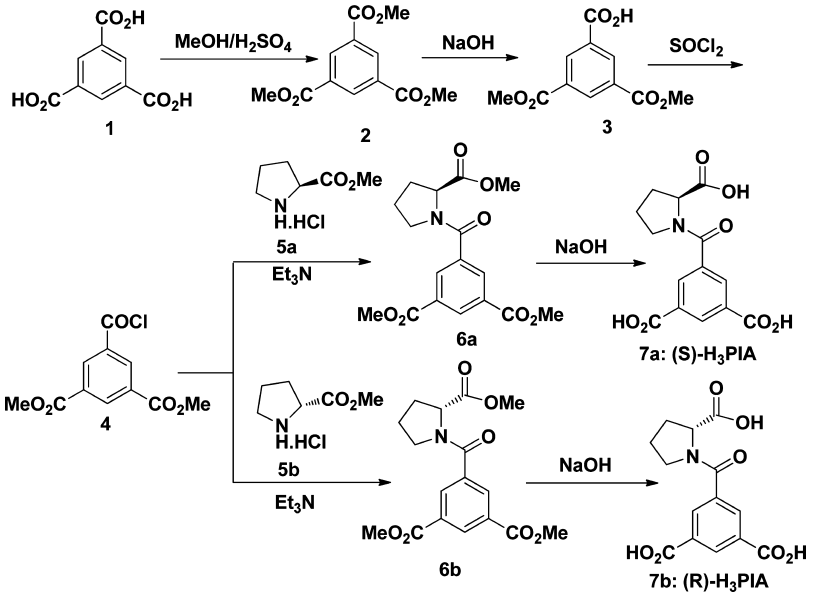

spectra. FT-IR spectra were measured as KBr pellets on a Nicolet Magna 750 FT-IR spectrometer in the range of 350−4000 cm^{-1}. All powder X-ray diffraction (PXRD) analyses were recorded on a Rigaku Dmax 2500 diffractometer with Cu Kα radiation (λ = 1.54056 Å). Thermal stability studies were carried out on a Netzsch Model STA-449C thermoanalyzer with a heating rate of 10 °C/min under an nitrogen atmosphere. Gas adsorption measurement was performed in the Micromeritics ASAP 2020 system.

Synthesis of Trimethyl-1,3,5-benzenetricarboxylate (2). Benzene-1,3,5-tricarboxylic acid (**1**) (21.0 g, 100 mmol) and concentrated sulfuric acid (5 mL) were dissolved in dry methanol (400 mL), and then the solution was refluxed for 24 h at 120 °C. After most of solvent was removed by rotary evaporation, the resulting residue was slowly added into saturated sodium bicarbonate (800 mL). The mixture was stirred at room temperature for 1 h, then filtered under reduced pressure to give the desired product, trimethyl-1,3,5-benzenetricarboxylate (compound **2**), as a white powder (22.7 g, 90%): ^{1}H NMR (400 MHz, $CDCl_3$), δ (ppm): 8.80 (3H, *s*), 3.96 (9H, *s*); ^{13}C NMR (100 MHz, $CDCl_3$), δ (ppm): 165.32, 134.51, 131.12, 52.62; LRSM (ESI): Mass calcd for $C_{12}H_{13}O_6$ $[M+H]^+$, 253.2; found 253.3.

Synthesis of 3,5-Bis(methoxycarbonyl)benzoic Acid (3). Compound **2** (10.1 g, 40 mmol) was dissolved in methanol (500 mL), then aqueous sodium hydroxide (35 mL, 35 mmol) was slowly added over a period of 24 h. After the mixture was stirred vigorously for 36 h, the solvent was moved by rotary evaporation. Sodium bicarbonate (10.6 g, 100 mmol) and water (200 mL) were added in the resulting residue, and the suspension was stirred for 2 h at 50 °C. The suspension was filtered under reduced pressure to get unreacted starting material (1.2 g, 4.8 mmol). After acidizing to pH 1.0 with concentrated HCl, the precipitated solid was separated by filtration to give pure 3,5-bis(methoxycarbonyl)benzoic acid (compound **3**) as a white powder (6.7 g, 70%): ^{1}H NMR (400 MHz, DMSO), δ (ppm): 13.68 (1H, *brs*), 8.59−8.51 (3H, *sss*), 3.91 (6H, *s*); ^{13}C NMR (100 MHz, DMSO), δ (ppm): 165.93, 165.05, 134.02, 133.45, 132.56, 131.13, 53.17; LRSM (ESI): Mass calcd for $C_{12}H_{11}O_6$ $[M+H]^+$, 239.2; found 239.4.

Synthesis of Dimethyl-5-(methoxycarbonyl)prrolidine-1-carbonyl)isophthalate (6). To a round-bottomed flask containing compound **3** (7.14 g, 30 mmol) and freshly distilled $SOCl_2$ (60 mL), four drops of dimethylformamide (DMF) was added under a nitrogen atmosphere. The reaction mixture was heated at 90 °C for 2 h, then the excess $SOCl_2$ was removed under in vacuo, giving dimethyl-5-(chlorocarbonyl)isophthalate (**4**) as a white solid. To a solution of methyl ester of L-proline or D-proline hydrochloride (**5**) (5.45 g, 33 mmol) in the dry CH_2Cl_2 (100 mL) and triethylamine (6.67 g, 66 mmol) under a nitrogen atmosphere and ice-water bath, compound **4** in dry CH_2Cl_2 (40 mL) was added dropwise over a period of 2 h. The reaction mixture was washed with 1.0 M HCl (2 × 30 mL) and saturated NaCl (2 × 30 mL), then dried over anhydrous sodium sulfate. After filtration and removal of the solvent in vacuo, the residue was purified by flash column chromatography (EtOAc:petroleum ether = 1:3) to give dimethyl-5-(methoxycarbonyl)prrolidine-1-carbonyl)-isophthalate (compound **6**) as an amber-colored oil (8.90 g, 85%): ^{1}H NMR (400 MHz, $CDCl_3$), δ (ppm): 8.8−8.25 (3H, *m*), 4.71−4.28 (1H, *m*), 3.96 (6H, *s*), 3.80−3.62 (3H, *ss*), 3.66−3.54 (2H, *m*), 2.37−2.33 (1H, *m*), 2.12−1.31 (4H, *m*); ^{13}C NMR (100 MHz, $CDCl_3$), δ (ppm): 172.38, 167.66, 165.49, 165.41, 136.31, 134.93, 132.46, 132.13, 131.80, 131.15, 130.94, 61.38, 59.32, 52.56, 52.39, 49.90, 46.85, 31.47, 29.34, 25.29, 22.65; LRSM (ESI): Mass calcd for $C_{12}H_{11}O_6$ $[M+H]^+$, 349.1; found 349.4.

Synthesis of 5-(2-carboxypyrrolidine-1-carbonyl)isophthalic Acid (7). Compound **6** (3.49 g, 10 mmol), methanol (10 mL), water (40 mL), and solid sodium hydroxide (1.8 g, 45 mmol) were added to a 100-mL round-bottomed flask containing a stirring bar. The reaction mixture was stirred and heated at 50 °C for 10 h, and then the result solution was slowly acidified to pH 1−2 with concentrated aqueous HCl in an ice bath. The precipitated solid was separated by filtration to give pure compound **7** (2.6 g, 8.5 mmol, 85%) as a white solid: ^{1}H NMR (400 MHz, DMSO), δ (ppm): 13.33 (3H, *brs*), 8.64−8.13 (3H, *m*), 4.46−4.30 (1H, *m*), 3.60−3.49 (2H, *m*), 2.51−2.28 (1H, *m*), 1.93−1.84 (3H, *m*); ^{13}C NMR (100 MHz, DMSO), δ (ppm): 173.96, 173.54, 167.06, 166.51, 166.42, 138.48, 137.66, 132.19, 132.04, 131.91, 131.68, 131.59, 131.10, 61.25, 59.50, 50.07, 47.01, 31.51, 29.42, 25.47, 22.79; LRSM (ESI): Mass calcd for $C_{12}H_{11}O_6$ $[M+H]^+$, 308.1; found 308.2.

Synthesis of [Cu_3((S)-PIA)$_2$(1.4-dioxane)(H_2O)$_2$]·(1.4-doxane)$_2$·H_2O (L-1). A mixture of (*S*)-H_3PIA (31 mg, 0.1 mmol) and $Cu(NO_3)_2$·2.5H_2O (47 mg, 0.2 mmol) was dissolved in a solvent mixture of 1.4-dioxane and H_2O (4 mL/1 mL) with two drops of pyridine in a screw-capped vial. The reaction mixture was heated at 100 °C for 3 days and then cooled to room temperature. Green-blue polygonal crystals (40 mg, 70%, based on (*S*)-H_3PIA) were obtained after filtration. Elemental analysis calcd (%) for **L-1**: C 43.05, H 4.48, N 2.51; found C 43.44, H 4.62, N 2.35. IR (solid KBr pellet, cm^{-1}): 3412.4*m*, 2360.7*w*, 1621.0*s*, 1442*m*, 1398*s*, 1363.6*s*, 1307.3*w*, 717.7*m*, 487.2*w*.

Synthesis of [Cu_3((R)-PIA)$_2$(1.4-dioxane)(H_2O)$_2$]·(1.4-doxane)$_2$·H_2O (D-1). The same procedure as that for **L-1** was used, except that (*R*)-H_3PIA was used instead of (*S*)-PIA). Green-blue polygonal crystals (42 mg, 73%, based on (R)-H_3PIA) were obtained after filtration. Elemental analysis calcd (%) for **L-1**: C 43.05, H 4.48, N 2.51; found C 43.61, H 4.67, N 2.45.

dx.doi.org/10.1021/ic501849g | *Inorg. Chem.* 2014, 53, 12199−12204

Table 1. Crystal Data and Structure Refinement for L-1, D-1, L-2, and D-2

compound reference	L-1	D-1	L-2	D-2
chemical formula	$C_{40}H_{51}Cu_3N_2O_{23}$	$C_{40}H_{51}Cu_3N_2O_{23}$	$C_{35}H_{35}Cu_4N_{2.5}O_{22.5}$	$C_{35}H_{35}Cu_4N_{2.5}O_{22.5}$
formula mass	1118.45	1118.45	1104.8	1104.8
crystal system	monoclinic	monoclinic	tetragonal	tetragonal
a (Å)	21.7630(6)	21.7800(3)	12.4736(1)	12.5085(1)
b (Å)	11.0749(4)	10.8551(1)	12.4736(1)	12.5085(1)
c (Å)	19.5074(5)	19.4405(3)	70.2884(8)	70.2284(15)
α (°)	90.00	90.00	90.00	90.00
β (°)	92.760(3)	92.0880(10)	90.00	90.00
γ (°)	90.00	90.00	90.00	90.00
unit-cell volume (Å^3)	4696.3(2)	4593.15(10)	10936.22(18)	10988.1(3)
temperature (K)	293(2)	293(2)	293(2)	293(2)
space group	$C2$	$C2$	$P4_12_12$	$P4_32_12$
Z	4	4	8	8
density, calcd. (g/cm^3)	1.572	1.617	1.332	1.326
radiation type	Mo Kα	Cu Kα	Cu Kα	Cu Kα
absorption coefficient (μ/mm^{-1})	1.432	2.384	2.372	2.361
$F(000)$	2276	2304	4376	4376
θ range data collection	2.74−25	2.27−76.57	3.60−74.61	2.52−74.62
No. of reflections measured	9329	22470	22338	22739
No. of independent reflections	6214	8781	10787	10680
R_{int}	0.0198	0.0292	0.0422	0.0398
final R_1 values ($I > 2\sigma(I)$)	0.0363	0.0359	0.0848	0.0874
final $wR(F^2)$ values ($I > 2\sigma(I)$)	0.0960	0.1136	0.2432	0.2544
final R_1 values (all data)	0.0414	0.0376	0.0894	0.0924
final $wR(F^2)$ values (all data)	0.1000	0.1186	0.2519	0.2620
goodness of fit on F^2	1.005	1.023	1.007	1.013
Flack parameter	−0.018(13)	−0.029(19)	0.00(1)	0.00(1)

*Synthesis of [Cu$_4$((S)-PIA)$_{2.5}$(H$_2$O)$_3$](guest) (**L-2**).* A mixture of (*S*)-H$_3$PIA (31 mg, 0.1 mmol) and Cu(NO$_3$)$_2$·2.5H$_2$O (47 mg, 0.2 mmol) was dissolved in a solvent mixture of *N*,*N*-diethylformamide and H$_2$O (1 mL/3 mL) in a screw-capped vial. The reaction mixture was heated at 100 °C for 3 days and then cooled to room temperature. Green-blue octahedral crystals (32 mg, 80%, based on (*S*)-H$_3$PIA) were obtained after filtration. Elemental analysis calcd (%) for **L-2**: C 41.19, H 2.45, N 3.43; found C 42.56, H 2.78, N 3.92. IR (solid KBr pellet, cm^{-1}): 3125.3*m*, 2968.9*w*, 2362.2*w*, 2337.3*w*, 1629.7*s*, 1586.6*m*, 1452.7*m*, 1370.3*s*, 1301.5*w*, 713.9*m*, 480.1*w*.

*Synthesis of [Cu$_4$((R)-PIA)$_{2.5}$(H$_2$O)$_3$](guest) (**D-2**).* The same procedure as that used for **L-2** was employed, except that (*R*)-H$_3$PIA was used instead of (*S*)-H$_3$PIA. Green-blue octahedral crystals (30 mg, 78%, based on (*R*)-H$_3$PIA) were obtained after filtration. Elemental analysis calcd (%) for **D-2**: C 41.19, H 2.45, N 3.43; found C 42.66, H 2.88, N 3.62.

X-ray Crystallographic Analysis. The diffraction data for the compounds were collected on an SuperNova diffractometer. The structures were solved by direct methods and refined on F^2 full-matrix least-squares using the SHELXTL-97 program package. All non-hydrogen atoms were refined anisotropically. Crystal data for the compounds are summarized in Table 1.

RESULTS AND DISCUSSION

Both **L-1** and **L-2** were synthesized solvothermally at the same reaction temperature, but different solvents were used to produce two distinct structures. The prominent structural feature of **L-1** is the packing of irregular cages building from [Cu$_2$(COO)$_4$] units and (*S*)-PIA ligands. Single-crystal X-ray diffraction (XRD) study confirmed that compound **L-1** crystallized in the chiral space group *C*2 with a Flack parameter of −0.018(13). In the structure of **L-1**, each (*S*)-PIA ligand is a μ_6-linker and connects three paddle wheel [Cu$_2$(COO)$_4$] units, while each [Cu$_2$(COO)$_4$] unit is surrounded by four (*S*)-PIA ligands (see Figure 1a). It is notable that there are two types of [Cu$_2$(COO)$_4$] units. One [Cu$_2$(COO)$_4$] unit has three carboxylate groups from three isophthalate parts and one carboxylate group from the proline part. Meanwhile, two apical sites of this [Cu$_2$(COO)$_4$] unit are located by two water molecules. Another [Cu$_2$(COO)$_4$] unit has C_2 symmetry and links to pairs of isophthalate parts, proline parts and 1,4-dioxane molecules. Interestingly, the (*S*)-PIA ligands alternately connect the [Cu$_2$(COO)$_4$] units into irregular cage-type substructures

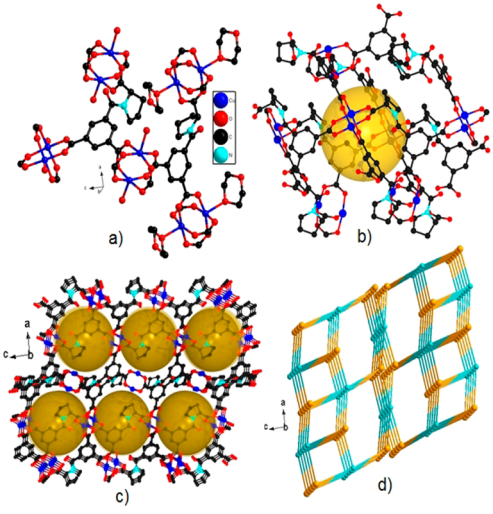

Figure 1. Schematic illustrations of **L-1**: (a) coordination environment; (b) cage substructure; (c) 3D framework, showing the packing of cages; and (d) topological net.

dx.doi.org/10.1021/ic501849g | *Inorg. Chem.* 2014, 53, 12199−12204

(see Figure 1b), and the cages are packing into a 3D porous framework (see Figure 1c). From the viewpoint of structural topology, the (*S*)-PIA ligands and the $[Cu_2(COO)_4]$ units can be regarded as the 3- and 4-connected nodes, respectively. Thus, the entire framework of **L-1** can be topologically represented as a (3,4)-connected net with point (Schläfli) symbol of $(4.8^2)_2(4.8^5)_2(8^3)_2(8^6)$ (see Figure 1d).

The outstanding structural feature of **L-2** compound is the presence of octahedral cages in the framework, which is unlike the irregular cages in **L-1**. Similar paddle wheel $[Cu_2(COO)_4]$ units are also the main inorganic building blocks in the structure of **L-2** (Figure 2a), and the (*S*)-PIA ligands link these

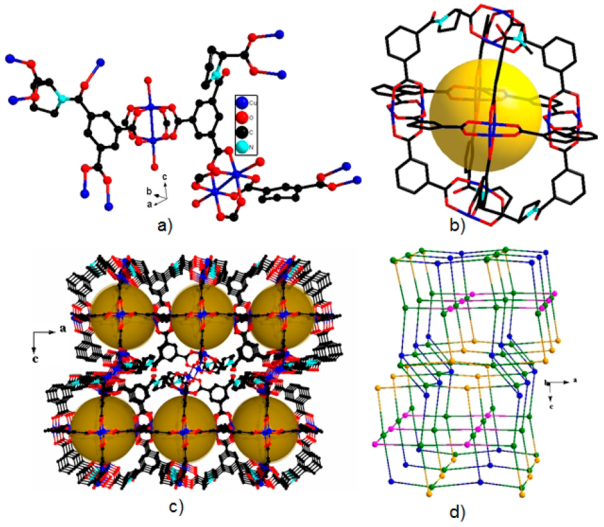

Figure 2. Schematic illustrations of **L-2**: (a) coordination environment; (b) cage substructure; (c) 3D framework, showing the packing of cages; and (d) topological net.

$[Cu_2(COO)_4]$ units into a 3D porous framework with octahedral cages (see Figures 2b and 2c). Each octahedral cage with an inner diameter of 7 Å consists of 12 (*S*)-PIA ligand fragments and 6 $[Cu_2(COO)_4]$ units (see Figure 2b). It is worthy of noting that one independent (*S*)-PIA ligand in the asymmetric unit of **L-2** is a μ_7-linker, with its acyl O atom bonding to one $[Cu_2(COO)_4]$ unit, so it acts as a 4-connected node in the topological representation and the related $[Cu_2(COO)_4]$ unit becomes a 5-connected node. Another independent (*S*)-PIA ligand and the secondary $[Cu_2(COO)_4]$ unit are the 3- and 4-connected nodes, respectively. Thus, the entire framework of **L-2** is topologically represented as a tetranodal (3,4,5)-connected net with point (Schläfli) symbol of $(4^2.6^3.8)_2(4^2.6^5.8^3)_2(6^2.8)_2(6^4.8^2)_3$ (Figure 2d).

Both **L-1** and **L-2** are porous frameworks and exhibit solvent-accessible volumes of ~43% and ~38%, as calculated by PLATON, respectively.[12] They are insoluble and stable in water and common organic solvents, such as methanol, ethanol, CH_2Cl_2, etc. (see Figures S4–S7 in the Supporting Information). The thermogravimetic analysis (TGA) indicated that both compounds also have high thermal stability (~240 °C) (see Figures S10 and S11 in the Supporting Information). The permanent porosity of **L-1** (or **L-2**) was further demonstrated by the N_2 gas sorption at 77 K. The desolvated samples of **L-1** and **L-2** show type-I sorption isotherms, respectively (see Figures S8 and S9 in the Supporting Information). The Langmuir and Brunauer–Emmett–Teller (BET) surface areas are 352.6 and 250.7 m^2/g for **L-1**, and 249.9 and 165.3 m^2/g for **L-2**, respectively.

Considering the presence of $[Cu_2(CO_2)_4]$ units with Lewis acid sites and chiral environment in these structures, further catalytic properties of these compounds were investigated. Here, we are interested in the catalytic synthesis of β-lactam through an oxidative carbon–carbon bond formation of phenolic amide derivatives. The β-lactam is not only observed in biologically active natural products, but also incorporated into numerous pharmaceutical ingredients, such as penicillins and carbapenems.[13] It is very important to create some new type of compounds containing a β-lactam unit for bacterial resistance. Although some homogeneous catalytic methods have been successfully applied to form β-lactam building blocks,[14] heterogeneous catalysis to fabricate this aim is still rarely explored up to date.

Since the carbon–carbon bond formation during the synthesis of β-lactam is largely dependent on proper oxidant and solvent, several oxidants (e.g., *tert*-butyl hydroperoxide (TBHP), H_2O_2, and iodobenzene diacetate (IBD)) and solvents (Table 2) are used to test the catalytic ability of two

Table 2. Optimization of the Catalyst[a]

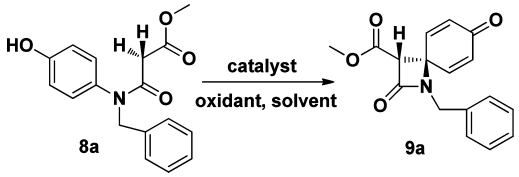

entry	catalyst	oxidant	solvent	temperature[b]	yield[c] (%)
1	**L-1**	IBD	ethanol	RT	56[d]
2	**L-1**	IBD	CH_3OH	RT	trace
3	**L-1**	IBD	acetone	RT	0
4	**L-1**	IBD	dioxane	RT	0
5	**L-1**	IBD	CH_2Cl_2	RT	0
6	**L-1**	IBD	ethanol	0 °C	58[d]
7	**L-1**	IBD	ethanol	50 °C	complexity
8		IBD	ethanol	RT	0
9	**D-1**	IBD	ethanol	RT	55[d]
10	**L-2**	IBD	ethanol	RT	trace
11	**HKUST-1**	IBD	ethanol	RT	trace

[a]Reactions were carried out at room temperature with amide **8a** (0.5 mmol), catalyst (0.025 mmol), and oxidant (0.6 mmol) in 10 mL of solvent for 3 h, except for entry 6, which was carried out at 0 °C for 10 h. [b]RT = room temperature. [c]On the basis of TLC detection. [d]Yields represent isolated yields of **9a**.

pairs of homochiral compounds. Our initial studies commenced with the reaction of compound **8a**. The results indicated that the reaction did not take place at all by using H_2O_2 or TBHP as the oxidizing agent in various solvents (see Table S3 in the Supporting Information). Fortunately, the IBD is effective in regard to promoting the reaction in ethanol at room temperature (Table 2, entry 1), giving product **9a** in moderate yield, but it still failed in other solvents (acetone, methanol, dioxane, and dichloromethane (DCM); see Table 2, entries 2–5). The efforts to enhance yields were also proved fruitless, when the reactions were conducted at lower or higher temperature (see Table 2, entries 6 and 7).

To demonstrate the heterogeneous nature of this catalytic system, compound **L-1** was stirred in ethanol for 3 h and removed by filtration, and then the reaction substrate (**8a**) and

dx.doi.org/10.1021/ic501849g | *Inorg. Chem.* 2014, 53, 12199–12204

oxidizing agent IBD were subsequently added into the filtrate and stirred for another 3 h at room temperature. As a result, only a trace of product **9a** was detected via thin-layer chromatography (TLC) (see Table 2, entry 8).

After being recovered using filtration and washed with ethanol, compound **L-1** could be subsequently used in the successive runs (see Figure S12 in the Supporting Information). The catalytic activity of **L-1** experienced only a slight degradation after four cycles; meanwhile, it always retained its crystallinity, as determined by PXRD (see Figure S13 in the Supporting Information). Encouraged by these results, both **L-2** and **HKUST-1** containing $[Cu_2(CO_2)_4]$ units were further screened under the same reaction condition, respectively. However, both of them cannot effectively catalyze the reaction (see Table 2, entries 10 and 11). These results might be correlated with the possible generation of Lewis acid sites from the $[Cu_2(CO_2)_4]$ units in the structures. For **L-1** (or **D-1**), the weak bond between the $[Cu_2(CO_2)_4]$ unit and 1,4-dioxane makes it easy to generate exposed Cu(II) sites for catalysis.

On the basis of the above results, the generality of this reaction was tested by a wide range of substituted phenol amides under the optimized condition. For catalyst **L-1**, the reaction has broad tolerance toward a variety of functional groups (see Table 3, compounds **8b**−**8l**). We found that the R_2 group of phenol amides had significant effects on the reaction.

Table 3. Substrate Scope[a]

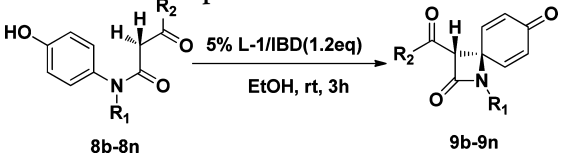

8b-8n 9b-9n

Amides	R_1	R_2	Yield[b]
8b → **9b**	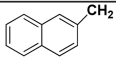	CH_3O	50%
8c → **9c**	$PhCH_2$	C_2H_5O	52%
8d → **9d**	m-$BrPhCH_2$	C_2H_5O	55%
8e → **9e**	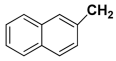	CH_3	62%
8f → **9f**	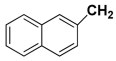	Ph	80%
8g → **9g**	$PhCH_2$	Ph	85%
8h → **9h**	*p*-NO_2PhCH_2	Ph	85%
8i → **9i**		Ph	78%
8j → **9j**	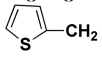	Ph	82%
8k → **9k**	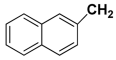	*p*-CH_3Ph	75%
8l → **9l**	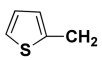	*p*-CH_3Ph	77%
8m → **9m**	*p*-CH_3Ph	*p*-NO_2Ph	trace[c]
8n → **9n**	*m*-NO_2PhCH_2	*p*-NO_2Ph	trace[c]

[a]The reaction was conducted with amide **8** (0.5 mmol), IBD (0.6 mmol) and **L-1** (0.025 mmol) in 10 mL C_2H_5OH at room temperature for 3 h. [b]Yields represent isolated yields of **9**. [c]On the basis of TLC detection.

With alkoxy or alkyl, the phenol amides only afforded the corresponding products in moderate yields under the standard reaction conditions (see Table 3, compounds **8b**−**8e**). When the R_2 group is phenyl or 4-methyl phenyl, the reaction performance is very efficient and all the yields are over 75% (see Table 3, **8f**−**8l**). However, phenol amides possessing a strong electron-withdrawing nitryl group on the phenyl ring afforded the products in trace amounts (see Table 3, compounds **7m**−**7n**). The screening of the R_2 groups revealed that various substituent groups, such as benzyl, *p*-methyl benzyl, *p*-nitryl benzyl, 2-methylene naphthalene, and so forth, were all suitable for the C−C bond coupling reaction.

Furthermore, crystals of compounds **8g**, **8i**, **8j**, and **8l** were successfully obtained after careful recrystallization, and their *β*-lactam structures were characterized by single-crystal X-ray diffraction (see Figure S3 and Table S2 in the Supporting Information). Because the large and small reagents showed similar reactivity, all these catalytic processes should take place on the surface of the catalyst **L-1**.[15]

CONCLUSION

In summary, two enantiopure organic ligands ((*S*)-H_3PIA and (*R*)-H_3PIA), integrating flexible proline units and rigid isophthalate units, have been rationally designed and employed to the construction of four homochiral porous MOFs (**L-1** and **D-1**, and **L-2** and **D-2**), respectively. Among them, **L-1** and **D-1** were used as heterogeneous catalysts for C−C oxidative coupling reaction. To the best of our knowledge, it is the first C−C oxidative forming procedure in the presence of porous MOFs. Further studies on the mechanistic aspects and applications of these compounds in organic synthesis are currently underway in our laboratory.

ASSOCIATED CONTENT

Supporting Information

^{1}H NMR, ^{13}C NMR spectra of all key intermediates, analytical data, and X-ray crystallographic files (CCDC-1011428−CCDC-1011431 (**L-1** and **D-1**, **L-2** and **D-2**) and CCDC-1011453−CCDC-1011456 (compounds **8g**, **8i**, **8j**, and **8l**)). This material is available free of charge via the Internet at http://pubs.acs.org.

AUTHOR INFORMATION

Corresponding Author

* E-mail: zhj@fjirsm.ac.cn.

Notes

The authors declare no competing financial interest.

ACKNOWLEDGMENTS

This work was supported by the 973 Program (Nos. 2012CB821705 and 2011CB932504) and NSFC (Nos. 21221001 and 21233009).

REFERENCES

(1) (a) Seo, J. S.; Whang, D.; Lee, H.; Jun, S. I.; Oh, J.; Jeon, Y. J.; Kim, K. *Nature* **2000**, *404*, 982−986. (b) Ma, L.; Abney, C.; Lin, W. B. *Chem. Soc. Rev.* **2009**, *38*, 1248−1256. (c) Yoon, M.; Srirambalaji, R.; Kim, K. *Chem. Rev.* **2012**, *112*, 1196−1231. (d) Liu, Y.; Xuan, W. M.; Cui, Y. *Adv. Mater.* **2010**, *22*, 4112−4235.

(2) (a) Xiong, R.-G.; You, X.-Z.; Abrahams, B. F.; Xue, Z.; Che, C.-M. *Angew. Chem., Int. Ed.* **2001**, *40*, 4422−4425. (b) Xi, X. B.; Fang, Y.; Dong, T. W.; Cui, Y. *Angew. Chem., Int. Ed.* **2011**, *50*, 1154−1158. (c) Mo, K.; Yang, Y. H.; Cui, Y. *J. Am. Chem. Soc.* **2014**, *136*, 1746−

1749. (d) Ma, L.; Falkowski, J. M.; Abney, C.; Lin, W. B. *Nat. Chem.* **2010**, *2*, 838−846. (e) Wang, C.; Liu, D. M.; Lin, W. B. *J. Am. Chem. Soc.* **2013**, *135*, 13222−13234. (f) Zhang, J.; Bu, X. H. *Angew. Chem., Int. Ed.* **2007**, *46*, 6115−6118. (g) Suh, K.; Yutkin, M. P.; Dybtsev, D. N.; Fedinc, V. P.; Kim, K. *Chem. Commun.* **2012**, *48*, 513−515. (h) Kang, Y.; Chen, S.; Wang, F.; Zhang, J.; Bu, X. *Chem. Commun.* **2011**, *47*, 4950−4952.

(3) (a) Dybtsev, D. N.; Nuzhdin, A. L.; Chun, H.; Bryliakov, K. P.; Talsi, E. P.; Fedln, V. P.; Kim, K. *Angew. Chem., Int. Ed.* **2006**, *45*, 916−920. (b) Vaidhyanathan, R.; Bradshaw, D.; Rebilly, J. N.; Barrio, J. P.; Gould, J. A.; Berry, N. G.; Rosseinsky, M. J. *Angew. Chem., Int. Ed.* **2006**, *45*, 6495−6499.

(4) (a) Zhang, J.; Chen, S. M.; Wu, T.; Feng, P. Y.; Bu, X. H. *J. Am. Chem. Soc.* **2008**, *130*, 12882. (b) Morris, R. E.; Bu, X. *Nat. Chem.* **2010**, *2*, 353−361. (c) Jing, X.; He, C.; Dong, D. P.; Yan, L. L.; Duan, C. Y. *Angew. Chem., Int. Ed.* **2012**, *51*, 10127−10131. (d) Appelhans, L. N.; Kosa, M.; Venkataramana, R.; Simoncic, P.; Navrotsky, A.; Parrinello, M.; Cheetham, A. K. *J. Am. Chem. Soc.* **2009**, *131*, 15375−15386.

(5) (a) Coma, A.; García, H.; Xamena, F. X. L. *Chem. Rev.* **2010**, *110*, 4606−4655. (b) Kreno, L. E.; Leong, K.; Farha, O. K.; Allendorf, M.; Duyne, R. P. V.; Hupp, J. T. *Chem. Rev.* **2012**, *112*, 1105−1125. (c) Tan, Y.-X.; He, Y.-P.; Zhang, J. *Chem. Mater.* **2012**, *24*, 4711−4716.

(6) (a) Dang, D. B.; Wu, P. Y.; He, C.; Xie, Z.; Duan, C. Y. *J. Am. Chem. Soc.* **2010**, *132*, 14321−14323. (b) Wu, P. Y.; He, C.; Wang, J.; Peng, X. J.; Li, X. Z.; An, Y. L.; Duan, C. Y. *J. Am. Chem. Soc.* **2012**, *134*, 14991−14999. (c) Han, Q. X.; He, C.; Zhao, M.; Qi, B.; Niu, J. Y.; Duan, C. Y. *J. Am. Chem. Soc.* **2013**, *135*, 10186−10189. (d) Lun, D. J.; Waterhouse, G. I. N.; Telfer, S. G. *J. Am. Chem. Soc.* **2011**, *133*, 5806−5809.

(7) (a) Rebilly, J.-N.; Bacsa, J.; Rosseinsky, M. J. *Chem.—Asian J.* **2009**, *4*, 892−903. (b) Ingleson, M. J.; Bacsa, J.; Rosseinsky, M. J. *Chem. Commun.* **2007**, *43*, 3036−3038. (c) Bai, S.; Sheng, T.; Tan, C.; Zhu, Q.; Huang, Y.; Jiang, H.; Hu, S.; Fu, R.; Wu, X. *J. Mater. Chem. A* **2013**, *1*, 2970−2973.

(8) (a) Kundu, T.; Sahoo, S. C.; Saha, S.; Banerjee, R. *Chem. Commun.* **2013**, *49*, 5262−5264. (b) Joarder, B.; Chaudhari, A. K.; Nagarkar, S. S.; Manna, B.; Ghosh, S. K. *Chem.—Eur. J.* **2013**, *19*, 11178−11183. (c) Lin, L.; Yu, R. M.; Yang, W. B.; Wu, X. Y.; Lu, C. Z. *Cryst. Growth. Des.* **2012**, *12*, 3304−3311. (d) Sahoo, S. C.; Kundu, T.; Banerjee, R. *J. Am. Chem. Soc.* **2011**, *133*, 17950−17958.

(9) Chui, S. S.-Y.; Lo, S. M.-F.; Chanmant, J. P. H.; Orpen, A. G.; Williams, I. D. *Science* **1999**, *283*, 1148−1150.

(10) Kumar, P.; Dwived, N. *Acc. Chem. Res.* **2013**, *46*, 289−299.

(11) (a) Perry, J. J., IV; Perman, J. A.; Zaworotko, M. J. *Chem. Soc. Rev.* **2009**, *38*, 1400−1417. (b) Liu, T.-F.; Chen, Y.-P.; Yakovenko, A. A.; Zhou, H.-C. *J. Am. Chem. Soc.* **2012**, *134*, 17358−17361. (c) Gao, W. Y.; Chen, Y.; Niu, Y. H.; Williams, K.; Cash, L.; Perez, P. J.; Wojtas, L.; Cai, J. F.; Cheng, Y. S.; Ma, S. Q. *Angew. Chem., Int. Ed.* **2014**, *126*, 2653−2657. (d) Opanasenko, M.; Shamzhy, M.; Céjka, J. *ChemCatChem* **2013**, *5*, 1024−1031.

(12) Spek, A. L. *J. Appl. Crystallogr.* **2003**, *36*, 7−13.

(13) Brown, E. D.; Wright, G. D. *Chem. Rev.* **2005**, *105*, 759−774.

(14) (a) Miyazawa, E.; Sakamoto, T.; Kikugawa, Y. *Heterocycles* **2003**, *53*, 149−154. (b) Wardrop, D. J.; Burge, M. S. *J. Org. Chem.* **2005**, *70*, 10271−10284. (c) Dohi, T.; Maruyma, A.; Minamitsuji, Y.; Takenaga, N.; Kita, Y. *Chem. Commun.* **2007**, *43*, 1224−1226. (d) Liang, J. X.; Cheng, J. B.; Du, F. X.; Zeng, X. H.; Li, L.; Zhong, H. B. *Org. Lett.* **2009**, *11*, 2820−2823.

(15) (a) Roberts, J. M.; Fini, B. M.; Sarjeant, A. A.; Farha, O. K.; Hupp, J. T. *J. Am. Chem. Soc.* **2012**, *134*, 3334−3337. (b) Lalonde, M. B.; Farha, O. K.; Scheidt, K. A.; Hupp, J. T. *ACS Catal.* **2012**, *2*, 1550−1554.